

Article

Farmed Chinese Perch (*Siniperca chuatsi*) Coinfected with Parasites and Oomycete Pathogens

Xiandong Xu ^{1,2,*}, Yanping Zhang ², Liyun Ding ², Jiangfeng Huang ², Zhiyong Zhou ² and Wenjing Chen ^{2,*}

¹ Education Ministry Key Laboratory of Poyang Lake Environment and Resource Utilization, College of Life Science, Nanchang University, Nanchang 330031, China

² Jiangxi Provincial Fisheries Research Institute, Nanchang 330039, China; zhangyanpingxie@163.com (Y.Z.); dingliyun2008@163.com (L.D.); hjf1992006@163.com (J.H.); zzy-88853@sohu.com (Z.Z.)

* Correspondence: xuxiandong2004@163.com (X.X.); wjchen87@126.com (W.C.); Tel./Fax: +86-791-8810-1682 (X.X.)

Abstract: Farming Chinese perch in aquaculture systems with artificial diets is a new method and developing trend. This method of raising Chinese perch has led to outbreaks of new diseases. In 2022, a disease outbreak occurred among farmed Chinese perch fed an artificial diet in Jiangxi Province, China, during which 50% of the fish died. The clinical signs exhibited by the diseased Chinese perch included decreased physical vitality, anorexia, emaciation, and dorsal fin ulceration with white cysts and flocs. Coinfection with ciliate parasites and an oomycete was found. No pathogenic bacteria were isolated from the microbial test, and the viral detection results were negative. After morphological and 18S or 28S rDNA sequence clustering analysis, the parasites were identified as *Epistylis wuhanensis* and *Zoothamnium* sp., while the oomycete was identified as *Achlya klebsiana*. This article discusses the interaction between parasitic and oomycete coinfections in Chinese perch from the perspective of the characteristics of Chinese perch raised with an artificial diet. The relationships between parasites, oomycete, and fish were also briefly discussed. This is the first report of the coinfection of Chinese perch with *Epistylis wuhanensis*, *Zoothamnium* sp. and *Achlya klebsiana*.

Keywords: Chinese perch; coinfections; *Epistylis wuhanensis*; *Zoothamnium* sp.; *Achlya klebsiana*

Key Contribution: In this study, the causes of severe disease in Chinese perch raised with artificial feed in aquaculture systems were investigated and analysed. Prevention and control methods are proposed.



Citation: Xu, X.; Zhang, Y.; Ding, L.; Huang, J.; Zhou, Z.; Chen, W. Farmed Chinese Perch (*Siniperca chuatsi*) Coinfected with Parasites and Oomycete Pathogens. *Fishes* **2024**, *9*, 97. <https://doi.org/10.3390/fishes9030097>

Received: 11 January 2024
Revised: 23 February 2024
Accepted: 29 February 2024
Published: 4 March 2024



Copyright: © 2024 by the authors. Licensee MDPI, Basel, Switzerland. This article is an open access article distributed under the terms and conditions of the Creative Commons Attribution (CC BY) license (<https://creativecommons.org/licenses/by/4.0/>).

1. Introduction

The Chinese perch (*Siniperca chuatsi*) is a rare freshwater fish in China. Its meat, without intermuscular spines, is delicious; therefore, it is very popular among consumers. Chinese perch farming yields large monetary benefits. In recent years, the market price has remained at more than USD 14 per kilogram, while that of grass carp (*Ctenopharyngodon idella*), the most farmed freshwater fish in China, is less than USD 2 per kilogram [1]. Chinese perch are widely farmed in the eastern and southern regions of China, with a production of 401,500 tons in 2022, accounting for 1.48% of freshwater farming [2]. In the wild, Chinese perch feed on live fry throughout their lives [3]. The traditional aquaculture of Chinese perch in China primarily involves pond farming, which typically relies on capturing rough fish from natural waters or artificially rearing prey fish such as mud carp (*Cirrhinus molitorella*). In the eastern region, fishing for rough fish remains a key component of Chinese perch farming. However, due to China's ban on fishing in natural waters, this practice has become unfeasible. Alternatively, mud carp have been specifically cultivated as prey fish in southern China. Nevertheless, the high costs associated with this method limit its widespread adoption. Additionally, feeding live fish bait increases the

risk of outbreaks of infectious diseases caused by bacterial and viral pathogens owing to horizontal transmission [4].

The use of an artificial diet for Chinese perch farming differs significantly from traditional methods utilizing live fish bait. This type of farming requires cement ponds or small water bodies with enclosed fisheries, ensuring that the farmed Chinese perch do not come into contact with external fish. This setup significantly reduces the risk of infectious diseases (bacterial or viral) under strict quarantine and prevention measures. Consequently, farming Chinese perch using an artificial diet has become a viable solution to the challenges associated with live fish feeding and has been implemented in several aquaculture farms in Chinese provinces, including Jiangxi, Hubei, and Guangdong [3,5]. However, a critical issue with this farming method is that the technology for the domestication of Chinese perch to eat artificial diet is not yet mature. If the domestication process fails, the Chinese perch will refuse to eat the artificial diet. Furthermore, this farming method generally employs nutrient-poor water with high stocking density [6,7], which makes the breeding of Chinese perch highly susceptible to outbreaks of new diseases. For instance, high mortality rates were observed in an aquaculture facility in Jiangxi Province, China that utilized an artificial diet. Therefore, our study investigated the cause of the disease-related mortalities. We provided morphological descriptions of parasites and oomycetes, conducted molecular identification, and analysed sections of Chinese perch gastrointestinal tissues and parasites. These findings serve as a reference for disease prevention and control measures in Chinese perch farms that utilize artificial diets.

2. Materials and Methods

2.1. Diseased Fish

In 2022, a disease broke out among farmed Chinese perch in cement ponds in Ji'an city, Jiangxi Province. The farmers reported purchasing Chinese perch fry measuring 80–100 mm and carrying out farming in September. After two weeks of farming, they noticed fish exhibiting clinical signs of illness, characterized by the appearance of white spots on their dorsal fins. After 2 months, the disease became more severe and led to 50% mortality. The farmers sought assistance and an investigation was promptly conducted. The size of the cement pond was 100 m², the water depth was 1.5 m, and the top of the pond was covered with shade sheds. About 3000 Chinese perch were reared in the cement pond with a commercial artificial diet (Jiangmen Yuewang Agricultural Technology Co., Ltd., Jiangmen, China) within shelf life. The aquaculture water source originated from upstream reservoirs, and the aquaculture water quality was clean. This water microflowed at a rate of 0.87 L/s. Upon examination, it was discovered that almost 80% of the remaining fish in the cement pond exhibited clinical signs, including decreased physical vitality, anorexia, emaciation, and dorsal fin ulceration with white cysts and flocs. A total of 20 fish (120–140 mm) with clinical signs which were assessed by visual examination were collected in a barrel with 100 L of pond water and sent to the laboratory for further photography and parasite and bacterial isolation and identification. Compressed air was pumped into the water using a battery-operated air pump, and the water temperature was maintained at approximately 17 °C during transportation. Transportation lasted for two hours.

2.2. Parasite and Pathogen Collection

A scalpel was used to scrape mucus from the skin (pectoral fin to caudal), fins, mouth, eyes, and gill tips for examination under a microscope. Cysts were observed on dorsal fins and tissue at cyst sites on the Chinese perch dorsal fins was obtained with scissors, placed in a flat dish containing deionized water, and observed under a dissecting microscope (Jiangnan SZ6100, Nanjing, China). Parasites were gently removed from the dorsal fins with a micropipette and transferred to another clean flat dish. Parasites were washed with deionized water by a micropipette, fin tissue debris was removed, and a portion of the parasite body was placed in a 1.5 mL sterile centrifuge tube, washed with 100 mL deionized water, and centrifuged (4000 r/min), and the supernatant was removed. The parasites were

fixed with absolute alcohol and stored at $-20\text{ }^{\circ}\text{C}$ for future DNA extraction. The remaining parasites were transferred to the centre of a slide, to which $20\text{ }\mu\text{L}$ of deionized water was added. A small amount of Vaseline was smeared on the four corners of the cover slide, the parasite was gently covered, the four corners were gently pressed with forceps, and the slide was placed under an Olympus microscope (40–200 times) for observation and imaging. Parasite identification and measurement data are presented as the mean \pm standard deviation. The Chinese perch were euthanized by the rapid cooling method [8] and dissected by a ventral approach, and bacteria were isolated using inoculation loops to harvest tissue samples from liver and kidney tissue plated on nutrient medium plates (10 g/L peptone, 3 g/L beef extract, 5 g/L NaCl, Beijing Land Bridge Technology, Beijing, China) cultivated at $28\text{ }^{\circ}\text{C}$ for 24 h.

2.3. Oomycete Isolation and Purification

Sterile forceps were used to obtain mycelium from Chinese perch and placed on a potato dextrose agar medium plate (Hope Bio-Technology, Qingdao, China) containing ampicillin. The plates were incubated at a constant temperature of $20\text{ }^{\circ}\text{C}$ for 48 h. A few mycelia were harvested from the plate and placed in potato dextrose water medium (Hope Bio-Technology, Qingdao, China). The cultures were incubated at a constant temperature of $20\text{ }^{\circ}\text{C}$ for 24 h. A small amount of liquid culture suspension was placed on the centre of a slide under a microscope (100 times) for observation and imaging. One hundred microlitres of suspension was aspirated, placed on a potato dextrose agar medium plate, smeared evenly, and incubated at a constant temperature of $20\text{ }^{\circ}\text{C}$ for 48 h. After the oomycete had grown into a single colony, a sterile scalpel was used to cut a single-colony agar block, which was subsequently placed on a potato glucose agar medium plate for purification and cultivation. The cultivation was carried out at $20\text{ }^{\circ}\text{C}$ for 48 h, after which the agar blocks were stored at $4\text{ }^{\circ}\text{C}$ for later use.

2.4. Histopathology

The dorsal fins with white cysts, stomach, intestines, liver, spleen, kidney, heart, brain, and gills of the euthanized Chinese perch were each sliced into small fragments (approximately 10 mm in length). These samples were then treated with a 4% paraformaldehyde solution at $4\text{ }^{\circ}\text{C}$ for 24 h. To serve as a control group, tissues from three healthy Chinese perches provided by the Jiangxi Provincial Fisheries Research Institute were extracted using the same method and tissue types as those of the euthanized fish. Dehydration, embedding, sectioning, and haematoxylin–eosin (H&E) staining were performed using conventional methods. Then, the samples were observed and photographed for parasite detection and description under a microscope (100–200 times).

2.5. DNA Extraction and Viral Detection

Parasites were preserved in absolute alcohol and collected by centrifugation for 5 min (4000 r/min), and the supernatant was removed. A Takara Universal Genomic DNA Extraction Kit (Takara Biotechnology (Dalian) Co., Ltd., Dalian, China) was used to extract the parasites, oomycetes, liver, and spleen tissue DNA following the manufacturer's instructions. The protease digestion time was extended until the liquid was clear. To extract oomycete DNA, sterile forceps were used to obtain a few purified and cultured oomycete mycelia, which were placed in a centrifuge tube. Sterile scissors were used to cut the mycelia as much as possible. For lysis, proteinase K and RNase were added, and the oomycete was lysed in a $56\text{ }^{\circ}\text{C}$ water bath. The lysis time was appropriately extended until the liquid became clear. Liver and spleen tissue RNA were extracted using the TaKaRa MiniBEST Universal RNA Extraction Kit (Takara Biotechnology (Dalian) Co., Ltd.). The common viral pathogens prevalent in Chinese perch, including iridovirus, infectious spleen and kidney necrosis virus, and rhabdovirus [9,10], were detected via commercial kit methods (DHelix, Guangzhou, China). Chinese perch liver and spleen tissue DNA were used for the purpose of detecting iridovirus and infectious spleen and kidney necrosis

virus, and the RNA were required for the detection of rhabdovirus. The detection of these viruses was conducted using a fluorescence quantitative PCR instrument (Mastercler Ep realplex4S, Eppendorf, Hamburg, Germany) according to the kit's instructions (DHelix, Guangzhou, China).

2.6. Cluster Analysis

For parasite 18S rDNA detection and sequencing, partial SSU rDNA sequences and all ITS1-5.8S-ITS2 regions were amplified using the ITSF/ITSR primer set [11]. The C1/D1 primer set [12] was used to amplify the oomycete 28S LSU rDNA. The primers used were synthesized by Sangon Biotech Co., Ltd. (Shanghai, China). The primer sequences and amplification conditions are shown in Table 1.

Table 1. Primers used for molecular characterization.

Prime	Protein or Virulent Factors	Primer Sequence (5' to 3')	Annealing Temperature (°C)	Amplicon Size (bp)	Reference
ITS	5.8S ribosomal RNA gene, and internal transcribed spacer 2	F:GTAGGTGAACCTGCGGAAG GATCATT R:TACTGATATGCTTAAGTTCA CGCG	50	500	[11]
C1/D1	28S large subunit ribosomal RNA gene	F:ACCCGCTGATTTAAGCAT R:TCCGTGTTTCAAGACGG	59	600	[12]

The polymerase chain reaction (PCR) mixture (25 µL) was composed of 12.5 µL of 2× Dream Taq Green PCR MasterMix (Thermo Scientific, Waltham, MA, USA), 1 µL of forward primer (10 µM), 1 µL of reverse primer (10 µM), 1 µL of template DNA, and ddH₂O (up to 25 µL). The PCR was conducted by a Mastercycler Nexus (Eppendorf, Germany) with cycle conditions as follows: predenaturation at 94 °C for 5 min; 35 cycles of amplification (94 °C for 45 s, suitable annealing temperatures for different primers at 50 °C or 59 °C for 30 s, and 72 °C for 30 s); and extension at 72 °C for 7 min [11,12].

After PCR amplification, the products were assessed via 1.5% agarose gel electrophoresis. If a target band was visible, the band was purified using the Rapid Agarose Gel DNA Recovery Kit [Takara Biotechnology (Dalian) Co., Ltd.]. The purified product was subsequently sent to Sangon Biotech Co., Ltd. (Shanghai, China) for sequencing, and the sequencing results were spliced and corrected via SeqMan software in the Lasergene v.7.1 (Madison, WI, USA) software package. BLAST was subsequently used to compare the sequences with those in the GenBank database, and sequences with a similarity greater than 97% were downloaded. MUSCLE comparisons within MEGA-X and phylogeny were performed to construct neighbour-joining clusters.

3. Results

3.1. Clinical Signs of Diseased Fish

In the affected cement pond, the average water temperature was 17 °C, the water pH was 6.3~7.2, the ammonia nitrogen concentration was 0.093 mg/L, the dissolved oxygen content was 5.4 mg/L, and the transparency was 1.5 m. The 20 collected fish were emaciated, appeared weak, and had white cysts and cotton-like masses on their dorsal fins (Figure 1A,C). Eight out of twenty fish exhibited collapsed eyeballs (Figure 1B). During the anatomical examination, there were no observable lesions in the internal organs, such as the liver, spleen, and kidneys. However, there was a notable absence of food in the stomach and intestines (Figure 1D). Additionally, no dominant bacteria were detected through microbiological analysis. The viral detection results were negative.

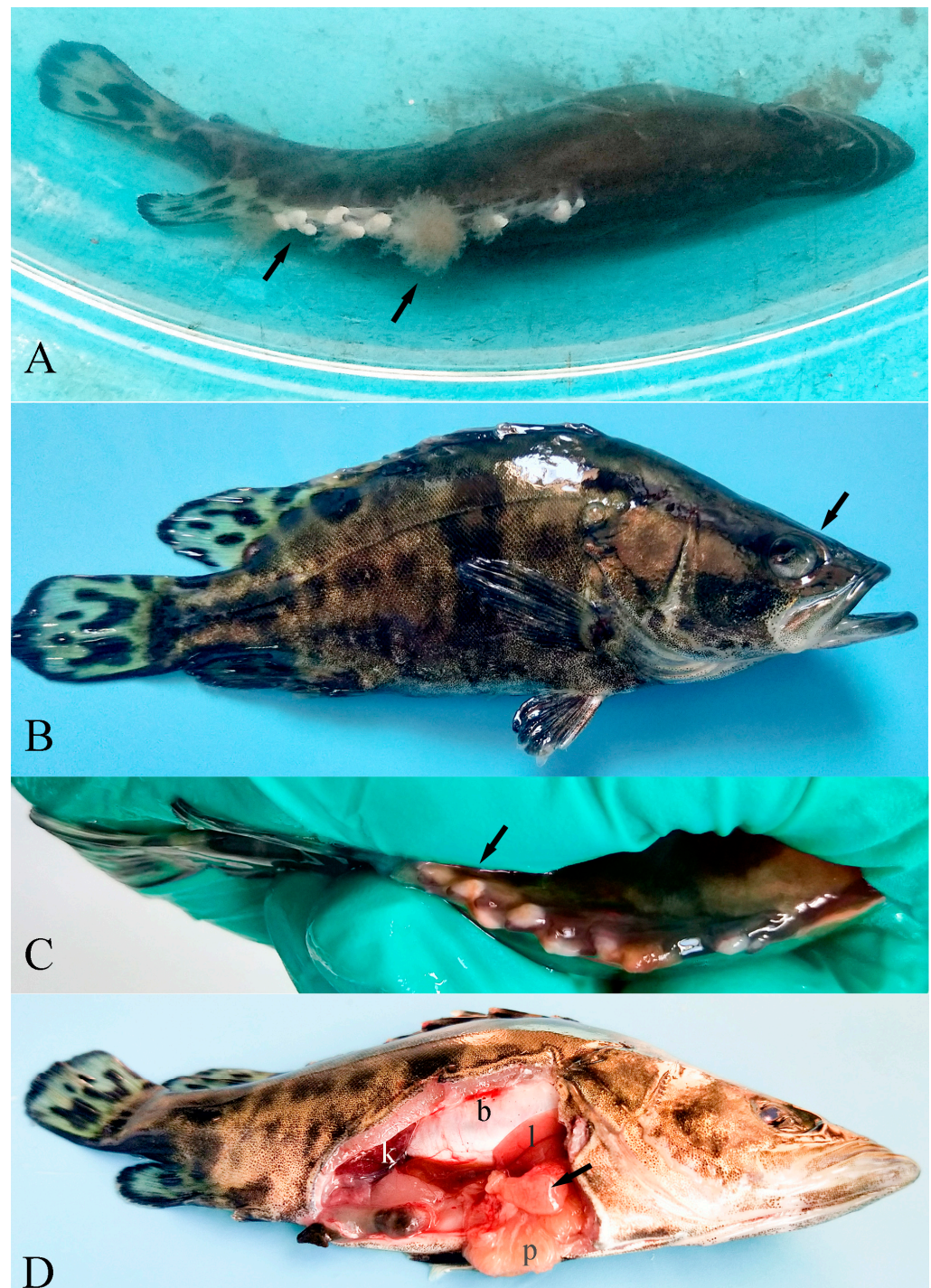


Figure 1. Clinical signs of infected Chinese perch. (A) Coinfected with oomycete and parasite, the arrow shows the flocs and the cyst formed by parasite infection. (B) Arrows indicate eye lesions, rupture of the eyeball, and collapse of the eye socket. (C) The dorsal fin of Chinese perch with white cysts (arrow); the clinical signs of flocs were difficult to detect with the naked eye after removing from the water. (D) Anatomical observation showed no obvious pathological changes in the liver (l), kidney (k), swim bladder (b), and pyloric caecum (p) of Chinese perch. The arrow indicates the absence of food in the gastrointestinal tract.

3.2. Parasite Morphology

No parasites were found on the gills, mouth, skin, or internal organs of the Chinese perch, but there were parasites on the fish with dorsal fins with white cysts and collapsed

eye sockets. Upon microscopic examination, we discovered that all 20 of the collected fish exhibited coinfections of parasites and an oomycete, and the oomycete hyphae mixed with parasites and debris (Figure 2A). There were two types of parasites. One was cylindrical, with an average body length of $254 \pm 21.3 \mu\text{m}$ and an average diameter of $52 \pm 4.6 \mu\text{m}$ in the extended state. It had a ring-shaped silverline system and two cilia on the oral disc. The cilia moved rapidly, forming a water flow that automatically flowed into the parasite's body to provide nutrients (Supplementary Materials Video S1). The stalk had no myoneme. Colonies of this type often dichotomously branched with two or more stalks, contained approximately 20 zooids, and were spherical after contraction. The swimmers were elliptical; therefore, these parasites were preliminarily identified as belonging to the genus *Epistylis* sp., a ciliate protozoan based on their morphological characteristics (Figure 2) [13]. The body of the second type of parasite was short and thick, with an average length of $103 \pm 8.7 \mu\text{m}$ and an average diameter of $85 \pm 6.8 \mu\text{m}$, and its stalk had filaments. It exhibited a Z-shaped contraction and was mushroom-like after contraction. There were a small number of individuals of this type in the collected fish samples. Therefore, these parasites were preliminarily identified as *Zoothamnium* sp., a ciliate protozoan. (Figure 3). Molecular analysis of the former parasites was also conducted, but molecular analysis was not conducted on the latter type of parasite because it was difficult to obtain pure individuals due to the small number of individuals.

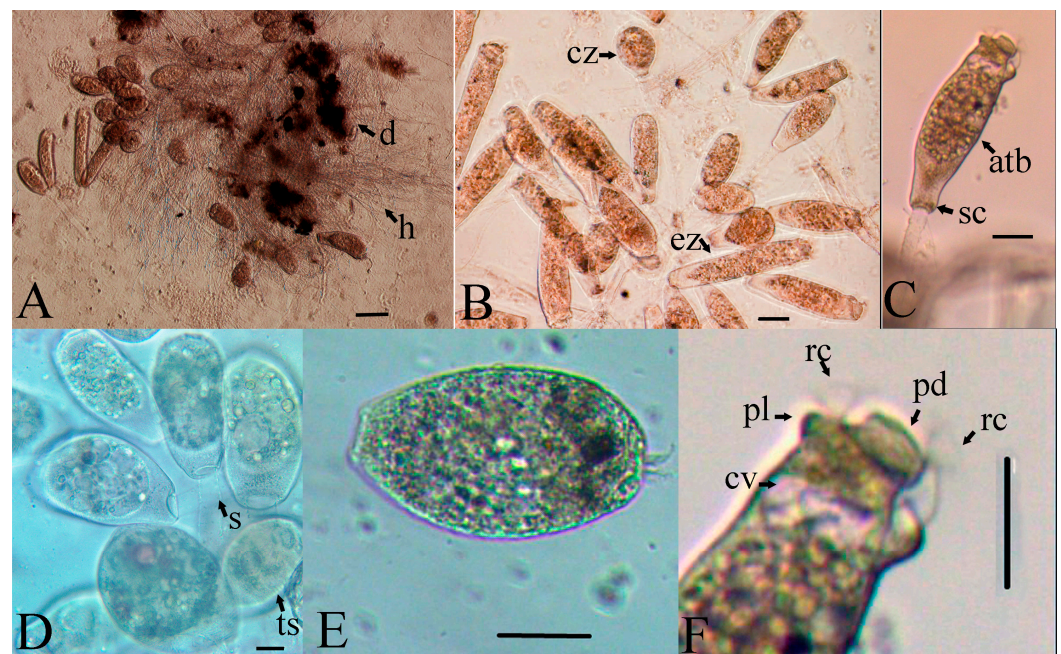


Figure 2. The morphology of *Epistylis* sp. and oomycete in vivo. (A) Coinfection of *Epistylis* sp. and oomycete, and oomycete hyphae mixed with parasites and debris; h, hyphae; d, debris. (B) The colony of *Epistylis* sp. zooids (100 times); ez, extended zooid; cz, contracted zooid. (C) An individual of *Epistylis* sp. zooid; atb, aboral trochal band; sc, scopula. (D) The colony of *Epistylis* sp. zooids (200 times); ts, transverse striations; s, stalk. (E) Larva of *Epistylis* sp. zooid. (F) The mouthparts of *Epistylis* sp.; pl, peristomial lip; pd, peristomial disk; rc, rotating cilia; cv, contractile vacuole. Scale bars: (A) = $50 \mu\text{m}$, (B–F) = $25 \mu\text{m}$.

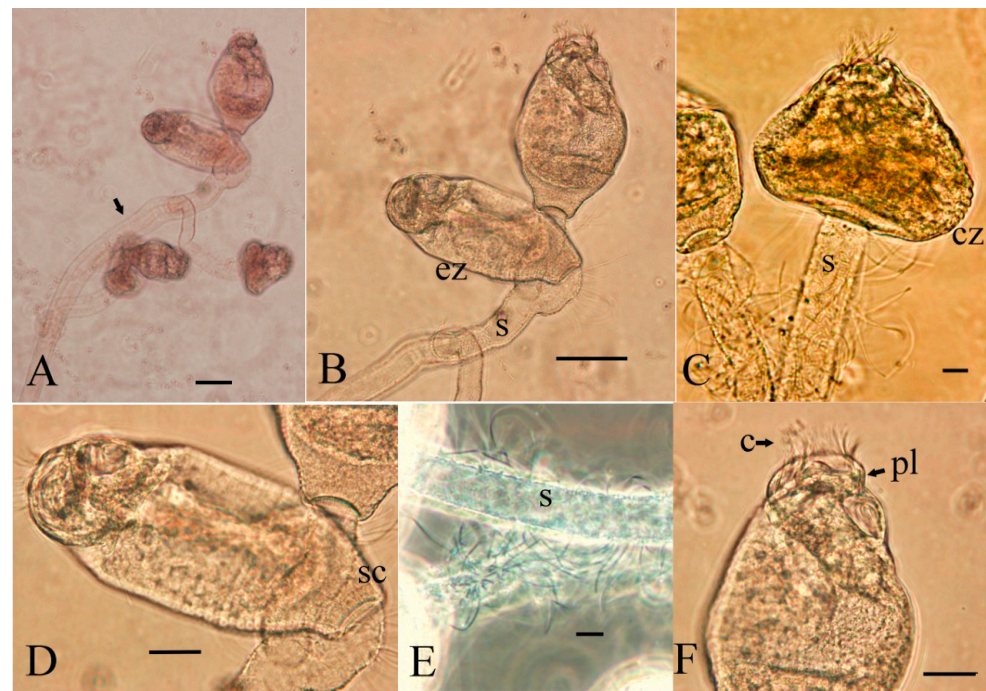


Figure 3. The morphology of *Zoothamnium* sp. in vivo. (A) A colony of *Zoothamnium* sp. zooids; the arrow shows Z-shaped contraction. (B) The extended zooids (ez); s, stalk. (C) The contracted zooids (cz); s, stalk. (D) A *Zoothamnium* sp. zooid individual; sc, scopula. (E) The stalk of *Zoothamnium* sp.; note the stalk (s) with myoneme. (F) The mouthparts of *Zoothamnium* sp.; c, cilia; pl, peristomial lip. Scale bars: (A,B) = 50 µm, (C–F) = 25 µm.

3.3. Oomycete Morphology

The oomycete hyphae in the parasitic state were hollow tubular structures, with sporangia arranged at intervals and spherical or pear-shaped egg collectors (Figure 4a). Under a microscope (100 times), oomycete hyphae were shown to be well developed, radiated from and diffused around the centre, and exhibited the morphological characteristics of *Achlya* (Figure 4b).

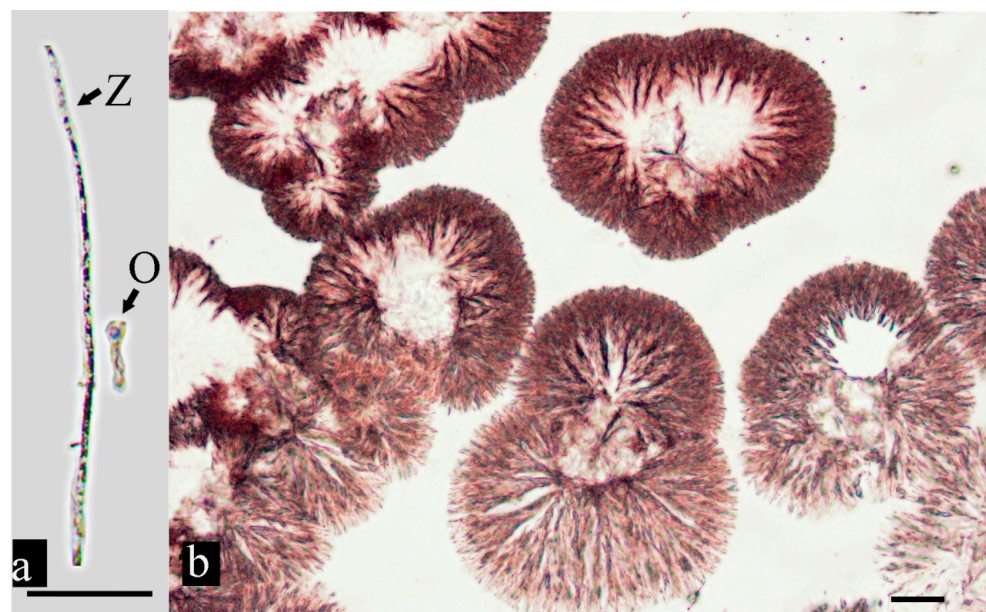


Figure 4. The morphology of oomycete in vivo (a) and under microscope (b). O, oogonium; Z, zoosporangia. Scale bars: 50 µm.

3.4. Tissue Histopathology

No significant pathological changes were observed in the liver, spleen, kidney, heart, brain, and gill tissues of the diseased fish (Supplementary Materials Figure S1). However, the infection site of the pathogen and the intestinal and gastric tissues displayed pathological alterations. Parasites were visible on the surfaces of the fin tissue. At the site of infection, it was evident that parasites had caused skin lesions (Figure 5A). Simultaneously, *E. wuhanensis* and *Zoothamnium* sp. could be observed (Figure 5B). The stalk of *Zoothamnium* sp. was accompanied by visible filaments. Notably, there were distinct disparities in the oral disc between the two parasite types. In the infected intestinal tissues of Chinese perch, the connection between the mucosal layer and the muscular layer connective tissues was loose, with local shedding and villus rupture and shedding (Figure 5D). The gastric tissue sections revealed a loose connection between the muscular layer and the submucosa, a disorderly arrangement of gastric epithelial cells, and striated border rupture (Figure 5F). No pathological changes were observed in the intestinal or gastric tissues of the normal Chinese perch (Figure 5C,E).

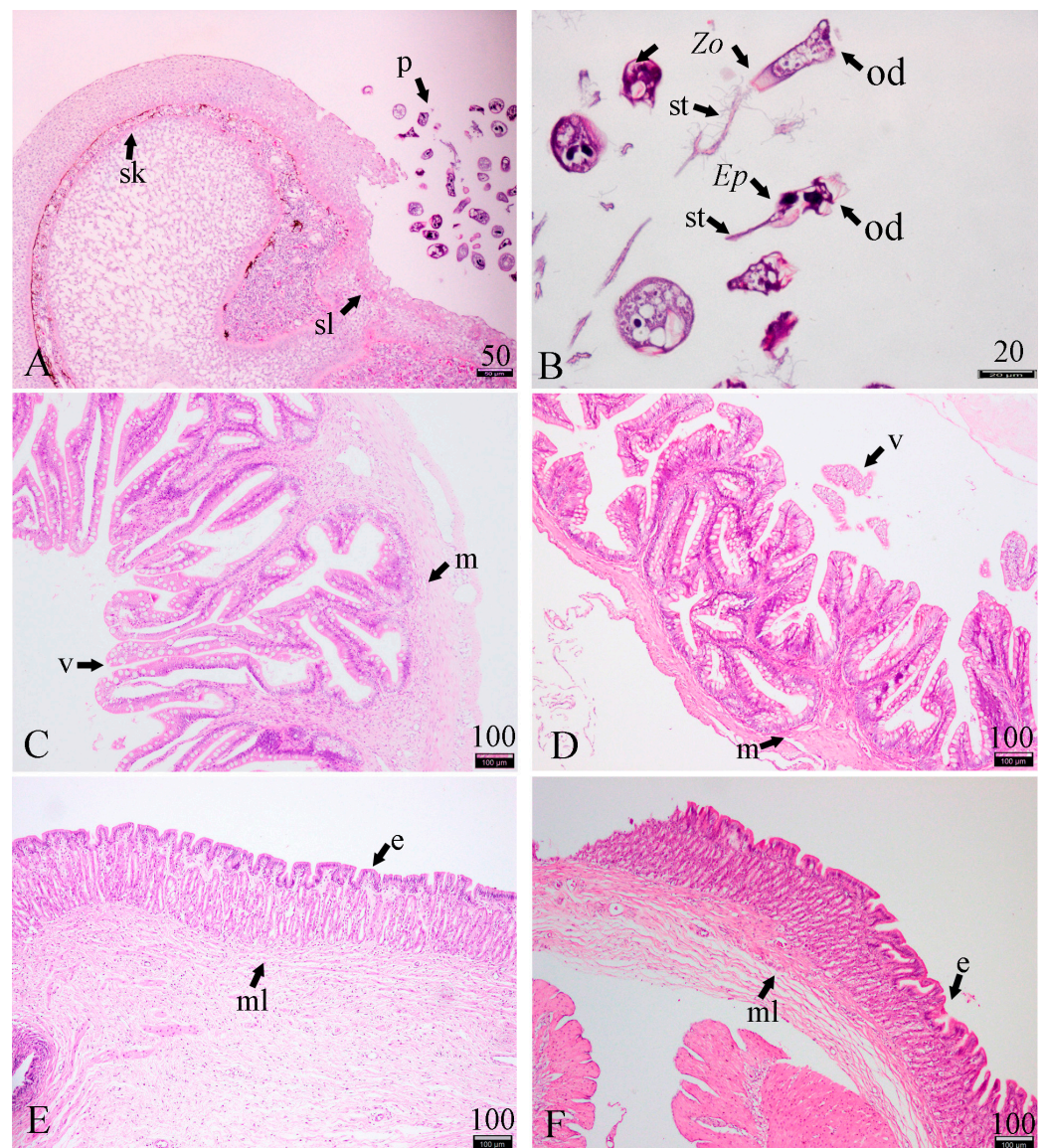


Figure 5. Histological sections (H & E) of Chinese perch coinfecting with parasite and oomycete. (A) Tissue sections of the infected sites (the dorsal fin of Chinese perch with white cyst); the arrow shows parasite infection, causing obvious skin lesions (sl) on the hosts; p, parasites; sk, skin. (B) The

tissue sections of parasites; *Ep*, *Epistylis wuhanensis*; *Zo*, *Zoothamnium* sp.; *st*, stalk; *od*, oral disk. (C) The intestinal tissue sections of healthy Chinese perch; *m*, mucosal layer; *v*, villus. (D) The intestinal tissue sections of the infected Chinese perch; the mucosal (*m*) layer and the muscular layer connective tissues were loose and shedding, while the villus (*v*) was ruptured and shedding. (E) The gastric tissue sections of healthy Chinese perch; *ml*, muscular layer; *e*, epithelial cells. (F) The gastric tissue sections of the infected Chinese perch, indicating a loose connection between the muscular layer (*mL*) and the submucosa, disorderly arrangement of gastric epithelial (*e*) cells, and striated border rupture. The number on the scale bars indicates the length of the scale bars in μm .

3.5. Sequence Alignment Analysis

A 317 bp sequence was obtained from the parasite DNA PCR amplification. The sequence was uploaded to GenBank (GenBank ID: OR141647). BLAST comparison revealed 100% similarity with the 5.8S ribosomal RNA gene and internal transcribed spacer 2 sequences of *E. wuhanensis*. Cluster analysis revealed that it clustered with *E. wuhanensis* (Figure 6). Based on morphological characteristics, the parasite was identified as *E. wuhanensis*. The 28S large subunit ribosomal RNA gene sequence of the fungus was 627 bp (login number OR141646). The oomycete sequence was highly similar to that of *Achlya klebsiana*, with a similarity of 100% to that of AF218191.1 and over 99.38% to that of other *A. klebsiana* sequences (Figure 7). Therefore, the oomycete was classified as *A. klebsiana*.

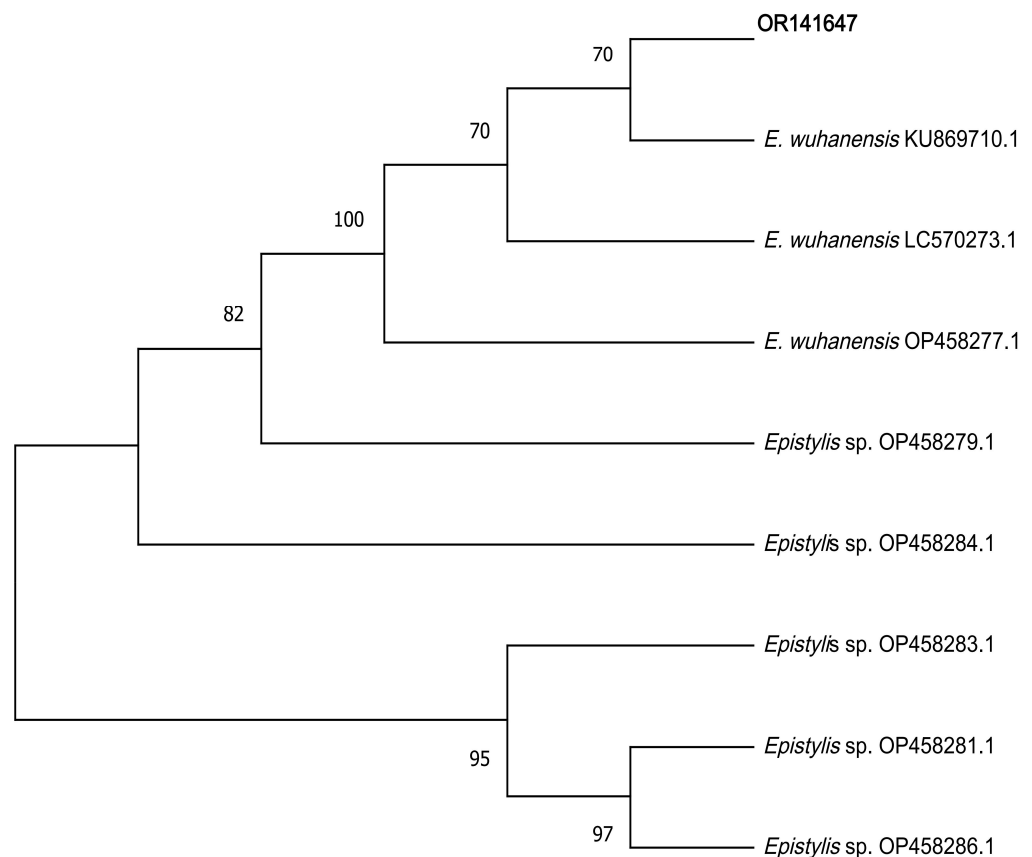


Figure 6. Phylogenetic tree of *Epistylis* sp. constructed from nuclear 18s rRNA gene sequences (neighbour-joining method).

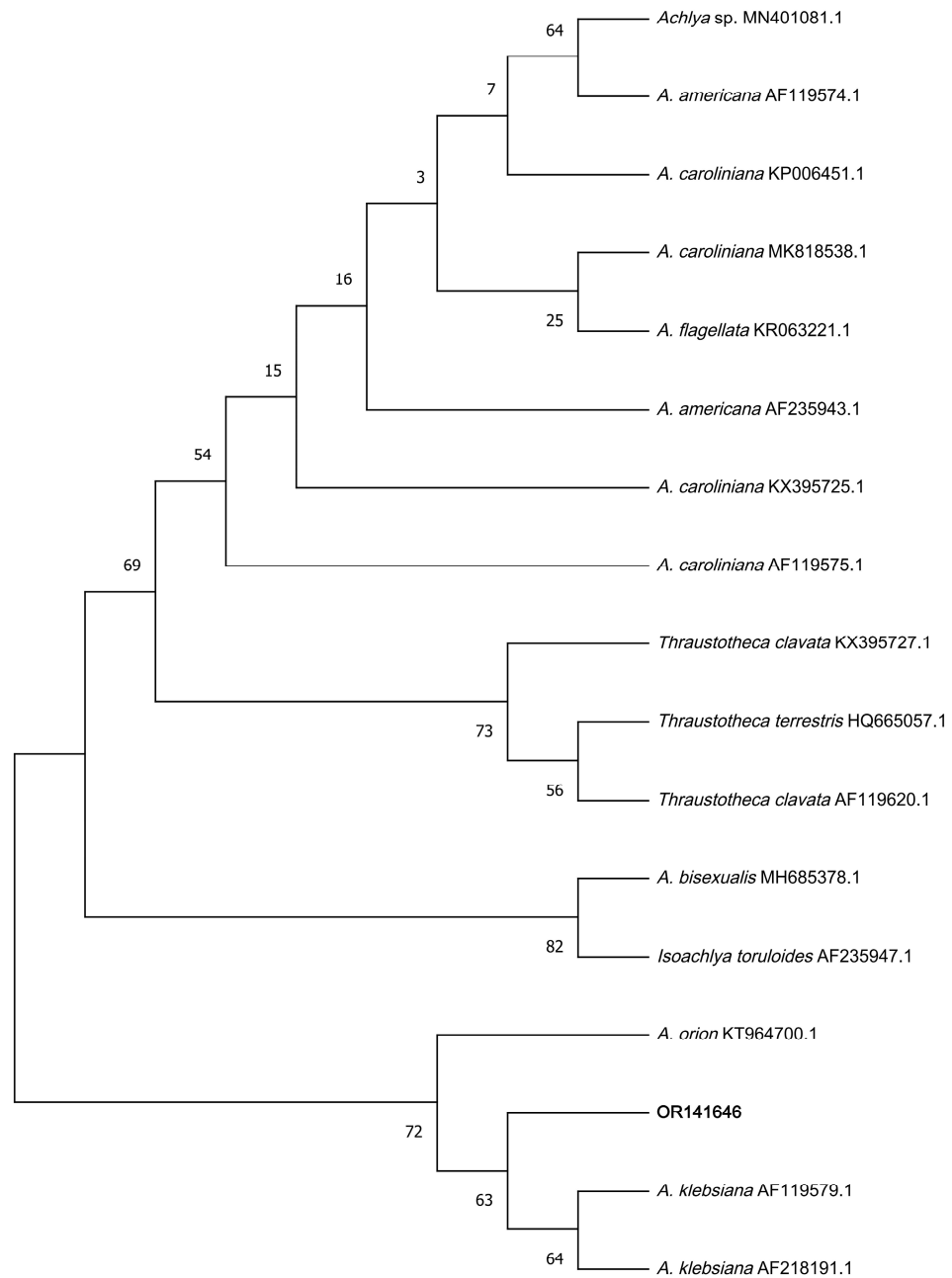


Figure 7. Phylogenetic tree of oomycete constructed from nuclear 28S rRNA gene sequences (neighbour-joining method).

4. Discussion

Chinese perch are rare freshwater fish in East Asia. They have a unique diet and feed on live fish bait throughout their life [14]. Traditionally, Chinese perch farming generally relies on live fish bait. However, the emergence of artificial diet-based farming represents a significant shift, offering a high-density, intensive method that avoids the use of live bait. Although this method is still in its infancy, with immature technology for domestication, it represents a future development trend of the Chinese perch farming industry [3–5]. Nonetheless, a challenge lies ahead in the form of Sessilida ciliate infections, which tend to spread during intensive culture conditions [13,15,16]. In the present study, Sessilida ciliates mainly parasitized the dorsal fins of Chinese perch, and generally, they did not directly cause death but rather allowed secondary oomycete infection. On the other hand, parasites that infect the eyes could cause ocular damage, potentially having a substantial impact on the survival of Chinese perch. Fish rely heavily on their eyes or lateral line scales to

sense prey and facilitate feeding [1]. Eye lesions could interfere with feeding, leading to hunger and damage to intestinal function. This, in turn, could seriously impede growth and ultimately result in the indirect death of the fish.

Coinfections in aquaculture are common, and there are multiple forms of coinfections [17,18]. For example, coinfections with the same type of pathogens include bacterial coinfections [19], viral coinfections [20], and parasitic coinfections [21]; coinfections with different types of pathogens include bacterial and viral [22]; parasitic and viral [23]; parasitic and bacterial [24]; and fungus and bacterial [25]. Coinfections of bacteria and multiple viruses in Chinese perch have been reported [10,13]; however, few parasitic coinfections and oomycete infections have been reported. To our knowledge, our study is the first to report a coinfection of Chinese perch with the ciliates *E. wuhanensis* and *Zoothamnium* sp., and the oomycete *A. klebsiana*.

Ciliates and oomycetes are both serious pathogens in aquaculture, and some of these pathogens have host specificity [15,16,26–30]. Accurately identifying types of parasites and oomycetes is important for understanding the pathogenesis, prevention, and control of diseases [14,26]. Traditional ciliate identification relies on methods such as microscopy (e.g., silver staining, protein staining, etc.) and analyses of zooid individual size measurements [13,29,31]. This process is tedious and prone to error, and identification is not always accurate [15]. Generally, identification is only possible at the genus level. The families *Epistylis* sp. and *Zoothamnium* sp. are extremely difficult to distinguish morphological types [32–35]. *Epistylis* sp. and *Zoothamnium* sp. species share similar morphologies and live in fixed populations that are connected by stalks between individuals [34]. The primary distinguishing feature between the two is that the stalks of *Epistylis* species do not include traction filaments and are incapable of contraction [35]. On the other hand, traditional oomycete identification primarily relies on morphological characteristics. This process can be challenging due to the diverse morphologies of oomycetes and the overlap in shapes among species [36]. Achieving accurate identification of these pathogens requires a combination of morphological and molecular biology methods [35,36].

This study identified coinfections of parasites and oomycete in Chinese perch. Drawing upon our observations and literature reports, which indicate that sessilids are harmful ectoparasites capable of degrading tissue at the attachment site, thus rendering wounds susceptible to fungal invasion [37,38], we hypothesized the existence of a synergistic relationship between parasites and oomycetes. Initially, parasites parasitize the dorsal fins of Chinese perch, causing surface damage (Figure 5A). Subsequently, the oomycete infects the wounds, during which mycelia grow into the muscles, obtain nutrients, and grow and reproduce to form mycelium clusters. The feed for Chinese perch is a high-protein diet rich in organic matter, which is prone to producing residual bait debris during feeding. As Figure 2A reveals, the oomycete mycelium clusters were accompanied by significant amounts of debris. This observation hints at the possibility that oomycete mycelium clusters may have retention and adhesion effects on organic debris. Parasites and oomycete mycelium clusters mix together, forming negative pressure through the high-speed rotation of cilia in the mouth, absorbing organic debris, obtaining rich nutrients, and reproducing and growing in large quantities (Supplementary Materials Video S1). In addition, Chinese perch are bottom-dwelling fish and do not like to move; a still-water environment is conducive to parasite–oomycete interactions. On this basis, we propose the following prevention and control suggestions for parasitic and oomycete coinfections in Chinese perch: Firstly, use flowing water aquaculture to increase the water flow velocity. Second, reduce feeding appropriately to curb the formation of residual bait or promptly remove residual feed.

5. Conclusions

The findings of our study revealed that coinfections with the ciliates *E. wuhanensis* and *Zoothamnium* sp., along with the oomycete *A. klebsiana*, resulted in the emergence of diseases among Chinese perch reared with artificial diets in fisheries within small water bodies.

To the best of our knowledge, our research presents the first report on the coinfections of Chinese perch by these ciliates and oomycete. Therefore, it is necessary to prioritize the prevention of such diseases in the cultivation of Chinese perch to minimize the losses attributed to coinfections.

Supplementary Materials: The following supporting information can be downloaded at: <https://www.mdpi.com/article/10.3390/fishes9030097/s1>, Video S1: The living state of the ciliates *E. wuhanensis*. Figure S1: Histological sections (H & E) of Chinese perch coinfecting with parasites and oomycete.

Author Contributions: Conceptualization, X.X. and W.C.; methodology, L.D.; software, Y.Z.; validation, L.D. and Y.Z.; formal analysis, J.H. and Z.Z.; investigation, X.X.; resources, X.X., L.D. and Y.Z.; data curation, X.X.; writing—original draft preparation, X.X.; writing—review and editing, W.C.; visualization, X.X.; supervision, W.C.; project administration, X.X. and Y.Z.; funding acquisition, X.X. and W.C. All authors have read and agreed to the published version of the manuscript.

Funding: This research was funded by the Natural Science Foundation of Jiangxi Province, grant number 20232BAB205070; the earmarked fund for the China Agriculture Research System, grant number CARS-46; the Key Research and Development Program of Jiangxi Province, grant numbers 20203BBFL63072, 20202BBFL63024, and the Breeding Research Project of Jiangxi Province, grant number 2023yyzgg-02.

Institutional Review Board Statement: The animal study protocol was approved by the Experimental Animal Ethics Committee of Nanchang University (approval code NCULAE-20230825136).

Data Availability Statement: All data generated or analysed during this study are included in the article and its supplementary information files.

Conflicts of Interest: The authors declare no conflicts of interest. The funders had no role in the design of the study; in the collection, analyses, or interpretation of data; in the writing of the manuscript; or in the decision to publish the results.

References

- Ren, Y.; Xiong, M.T.; Yu, J.X.; Li, W.; Li, B.; Liu, J.H.; Zhang, T.L. Effects of artificial submersed vegetation on consumption and growth of mandarin fish *Siniperca chuatsi* (Basilewsky) foraging on live prey. *J. Freshw. Ecol.* **2019**, *34*, 433–444. [\[CrossRef\]](#)
- Fisheries and Fisheries Administration of the Ministry of Agriculture and Rural Affairs of the People's Republic of China. *China Fishery Statistical Yearbook*; China Agriculture Press: Beijing, China, 2023. Available online: <https://www.stats.gov.cn/sj/nds/2023/index.htm> (accessed on 11 January 2024).
- He, S.; You, J.J.; Liang, X.F.; Zhang, Z.L.; Zhang, Y.P. Transcriptome sequencing and metabolome analysis of food habits domestication from live prey fish to artificial diets in mandarin fish (*Siniperca chuatsi*). *BMC Genom.* **2021**, *22*, 129. [\[CrossRef\]](#)
- Chen, X.L.; Yi, H.D.; Liu, S.; Zhang, Y.; Su, Y.Q.; Liu, X.G.; Bi, S.; Lai, H.; Zeng, Z.Y.; Li, G.F. Promotion of pellet-feed feeding in mandarin fish (*Siniperca chuatsi*) by *Bdellovibrio bacteriovorus* is influenced by immune and intestinal flora. *Aquaculture* **2021**, *52*, 736864. [\[CrossRef\]](#)
- Shen, Y.W.; Li, H.Y.; Zhao, J.L.; Tang, S.J.; Zhao, Y.; Bi, Y.H.; Chen, X.W. The digestive system of mandarin fish (*Siniperca chuatsi*) can adapt to domestication by feeding with artificial diet. *Aquaculture* **2021**, *538*, 736546. [\[CrossRef\]](#)
- Ruyet, J.P.; Labbé, L.; Le Bayon, N.; Sévère, A.; Le Roux, A.; Le Delliou, H.; Quémener, L. Combined effects of water quality and stocking density on welfare and growth of rainbow trout (*Oncorhynchus mykiss*). *Aquat. Living Resour.* **2008**, *21*, 185–195. [\[CrossRef\]](#)
- Birolo, M.; Bordignon, F.; Trocino, A.; Fasolato, L.; Pascual, A.; Godoy, S.; Nicoletto, C.; Maucieri, C.; Xiccato, G. Effects of stocking density on the growth and flesh quality of rainbow trout (*Oncorhynchus mykiss*) reared in a low-tech aquaponic system. *Aquaculture* **2020**, *529*, 735653. [\[CrossRef\]](#)
- Wilson, J.M.; Bunte, R.M.; Carty, A.J. Evaluation of rapid cooling and tricaine methanesulfonate (MS222) as methods of euthanasia in zebrafish (*Danio rerio*). *J. Am. Assoc. Lab. Anim. Sci.* **2009**, *48*, 785–789.
- Lin, Q.; Fu, X.; Li, N.; Wan, Q.; Chen, W.; Huang, Y.; Huang, Z.; Li, J.; Zhao, L.; Lin, L. Co-infections of infectious spleen and kidney necrosis virus and *Siniperca chuatsi* rhabdovirus in Chinese perch (*Siniperca chuatsi*). *Microb. Pathog.* **2017**, *111*, 422–430. [\[CrossRef\]](#)
- Liu, X.; Sun, W.; Zhang, Y.; Zhou, Y.; Xu, J.; Gao, X.; Zhang, S.; Zhang, X. Impact of *Aeromonas hydrophila* and infectious spleen and kidney necrosis virus infections on susceptibility and host immune response in Chinese perch (*Siniperca chuatsi*). *Fish Shellfish Immunol.* **2020**, *105*, 117–125. [\[CrossRef\]](#)

11. Yi, Z.; Song, W.; Clamp, J.C.; Chen, Z.; Gao, S.; Zhang, Q. Reconsideration of systematic relationships within the order Euplotida (Protista, Ciliophora) using new sequences of the gene coding for small-subunit rRNA and testing the use of combined data sets to construct phylogenies of the *Diophrys*-complex. *Mol. Phylogenet. Evol.* **2009**, *50*, 599–607. [[CrossRef](#)]
12. Leclerc, M.C.; Guillot, J.; Deville, M. Taxonomic and phylogenetic analysis of Saprolegniaceae (Oomycetes) inferred from LSU rDNA and ITS sequence comparisons. *Anton. Leeuw.* **2000**, *77*, 369–377. [[CrossRef](#)]
13. Wang, Z.; Zhou, T.; Guo, Q.; Gu, Z. Description of a New Freshwater Ciliate *Epistylis wuhanensis* n. sp. (Ciliophora, Peritrichia) from China, with a Focus on Phylogenetic Relationships within Family Epistylididae. *J. Eukaryot. Microbiol.* **2017**, *64*, 394–406. [[CrossRef](#)]
14. He, S.; Li, L.; Lv, L.Y.; Cai, W.J.; Dou, Y.Q.; Li, J.; Tang, S.L.; Chen, X.; Zhang, Z.; Xu, J.; et al. Mandarin fish (*Siniperca*) genomes provide insights into innate predatory feeding. *Commun. Biol.* **2020**, *3*, 361. [[CrossRef](#)]
15. Zhou, T.; Wang, Z.; Yang, H.; Gu, Z. Morphological and molecular identification of epibiotic sessile *Epistylis semiciculus* n. sp. (ciliophora, Peritrichia) from *Procambarus clarkia* (Crustacea, Decapoda) in China. *Int. J. Parasitol. Parasites Wildl.* **2019**, *10*, 289–298. [[CrossRef](#)]
16. Ksepka, S.P.; Bullard, S.A. Morphology, phylogenetics and pathology of “red sore disease” (coinfection by *Epistylis* cf. *wuhanensis* and *Aeromonas hydrophila*) on sportfishes from reservoirs in the South-Eastern United States. *J. Fish Dis.* **2021**, *44*, 541–551. [[CrossRef](#)]
17. Kotob, M.H.; Menanteau-Ledouble, S.; Kumar, G.; Abdelzaher, M.; El-Matbouli, M. The impact of co-infections on fish: A review. *Vet. Res.* **2017**, *47*, 98. [[CrossRef](#)]
18. Paul, A.; Pattanayak, S.; Sahoo, M.; Kumar, P.R.; Kumar, R.; Sahoo, P.K. Co-infection of bacterial and parasitic pathogens including the myxosporean *Zschokkella auratis* infecting brain in farmed striped murrel *Channa striata* (Bloch, 1793) causing large scale mortality. *Indian J. Fish.* **2020**, *67*, 105–115. [[CrossRef](#)]
19. Pu, W.; Guo, G.; Yang, N.; Li, Q.; Yin, F.; Wang, P.; Zheng, J.; Zeng, J. Three species of *Aeromonas* (*A. dhakensis*, *A. hydrophila* and *A. jandaei*) isolated from freshwater crocodiles (*Crocodylus siamensis*) with pneumonia and septicemia. *Let. Appl. Microbiol.* **2019**, *68*, 212–218. [[CrossRef](#)] [[PubMed](#)]
20. Alonso, M.; Rodríguez Saint-Jean, S.; Pérez-Prieto, S.I. Virulence of infectious hematopoietic necrosis virus and Infectious pancreatic necrosis virus coinfection in rainbow trout (*Oncorhynchus mykiss*) and nucleotide sequence analysis of the IHNV glycoprotein gene. *Arch. Virol.* **2003**, *148*, 1507–1521. [[CrossRef](#)]
21. Klemme, I.; Louhi, K.R.; Karvonen, A. Host infection history modifies co-infection success of multiple parasite genotypes. *J. Anim. Ecol.* **2016**, *85*, 591–597. [[CrossRef](#)]
22. Huang, Y.C.; Cai, S.H.; Jian, J.C.; Liu, G.F.; Xu, L.W. Co-infection of infectious spleen and kidney necrosis virus and *Francisella* sp. in farmed pearl gentian grouper (♀*Epinephelus fuscoguttatus* × ♂*E. lanceolatus*) in China—A case report. *Aquaculture* **2020**, *526*, 735409. [[CrossRef](#)]
23. Ogut, H.; Cavus, N. A comparison of ectoparasite prevalence and occurrence of viral haemorrhagic septicemia virus (VHSV) in whiting *Merlangius merlangus* euxinus. *Rev. Biol. Mar. Oceanog.* **2014**, *49*, 91–96. [[CrossRef](#)]
24. Densmore, C.I.; Ottinger, C.A.; Blazer, V.S.; Iwanowicz, L.R.; Smith, D.R. Immunomodulation and disease resistance in postyearling rainbow trout infected with *Myxobolus cerebralis*, the causative agent of whirling disease. *J. Aquat. Anim. Health* **2004**, *16*, 73–82. [[CrossRef](#)]
25. Cutuli, M.T.; Gibello, A.; Rodriguez-Bertos, A.; Blanco, M.M.; Villarreal, M.; Giraldo, A.; Guarro, J. Skin and subcutaneous mycoses in tilapia (*Oreochromis niloticus*) caused by *Fusarium oxysporum* in coinfection with *Aeromonas hydrophila*. *Med. Mycol. Case Rep.* **2015**, *9*, 7–11. [[CrossRef](#)]
26. Phillips, A.J.; Anderson, V.L.; Robertson, E.J.; Secombes, C.J.; van West, P. New insights into animal pathogenic oomycetes. *Trends Microbiol.* **2008**, *16*, 13–19. [[CrossRef](#)]
27. Gozlan, R.E.; Marshall, W.L.; Lilje, O.; Jessop, C.N.; Gleason, F.H.; Andreou, D. Current ecological understanding of fungal-like pathogens of fish: What lies beneath? *Front. Microbiol.* **2014**, *5*, 62. [[CrossRef](#)]
28. Jones, S.; Carrasco, N.K.; Perissinotto, R.; Vosloo, A. Association of the epibiotic *Epistylis* sp. with a calanoid copepod in the St Lucia Estuary, South Africa. *J. Plankton Res.* **2016**, *38*, 1404–1411. [[CrossRef](#)]
29. Kühner, S.; Simão, T.L.; Safi, L.S.; Gazulha, F.B.; Eizirik, E.; Utz, L.R. *Epistylis portoalegrensis* n. sp. (Ciliophora, Peritrichia): A New Freshwater Ciliate Species from Southern Brazil. *J. Eukaryot. Microbiol.* **2016**, *63*, 93–99. [[CrossRef](#)]
30. Borah, N.; Albarouki, E.; Schirawski, J. Comparative Methods for Molecular Determination of Host-Specificity Factors in Plant-Pathogenic Fungi. *Int. J. Mol. Sci.* **2018**, *19*, 863. [[CrossRef](#)]
31. Shi, X.; Meng, Q.; Liu, G.; Qi, G.; Jiang, C.; Meng, X.; Warren, A. Morphology and morphogenesis of *Epistylis plicatilis* ehrenberg, 1831 (Ciliophora, Peritrichia) from Wuhan, China. *J. Morphol.* **2014**, *275*, 882–893. [[CrossRef](#)] [[PubMed](#)]
32. Miao, W.; Yu, Y.H.; Shen, Y.F. Phylogenetic relationships of the subclass Peritrichia (Oligohymenophorea, Ciliophora) with emphasis on the genus *Epistylis*, inferred from small subunit rRNA gene sequences. *J. Eukaryot. Microbiol.* **2001**, *48*, 583–587. [[CrossRef](#)] [[PubMed](#)]
33. Miao, W.; Fen, W.; Yu, Y.; Zhang, X.; Shen, Y. Phylogenetic relationships of the subclass Peritrichia (Oligohymenophorea, Ciliophora) inferred from small subunit rRNA gene sequences. *J. Eukaryot. Microbiol.* **2004**, *51*, 180–186. [[CrossRef](#)]
34. Lynn, D. *The Ciliated Protozoa: Characterization, Classification, and Guide to the Literature*; Springer: Berlin/Heidelberg, Germany, 2008. [[CrossRef](#)]

35. Wang, Z.; Zhou, T.; Yang, H.; Gu, Z.M. First diagnosis of ectoparasitic ciliates (Trichodina and Chilodonella) on farmed juvenile yellow catfish, *Tachysurus fulvidraco* in China. *Aquac. Res.* **2019**, *50*, 14285. [[CrossRef](#)]
36. Choi, Y.J.; Lee, S.H.; Nguyen, T.; Nam, B.; Lee, H.B. Characterization of *Achlya americana* and *A. bisexualis* (Saprolegniales, Oomycota) isolated from freshwater environments in Korea. *Mycobiology* **2019**, *2*, 135–142. [[CrossRef](#)]
37. O’Keeffe, K.R.; Halliday, F.W.; Jones, C.D.; Carbone, I.; Mitchell, C.E. Parasites, niche modification and the host microbiome: A field survey of multiple parasites. *Mol. Ecol.* **2021**, *30*, 2404–2416. [[CrossRef](#)] [[PubMed](#)]
38. Li, M.; Li, W.; Ge, X.; Wang, C.; Zhang, L.; Huang, F.; Liu, H. First report of *Epistylis unioi* Gong 1986 (Sessilida: Epistylididae) infecting fry of *Pelteobagrus fulvidraco* in Hubei, China. *Zootaxa* **2012**, *3556*, 80–88. [[CrossRef](#)]

Disclaimer/Publisher’s Note: The statements, opinions and data contained in all publications are solely those of the individual author(s) and contributor(s) and not of MDPI and/or the editor(s). MDPI and/or the editor(s) disclaim responsibility for any injury to people or property resulting from any ideas, methods, instructions or products referred to in the content.